AD-A172 552 APPLICATIONS OF THE FINITE-ELEMENT METHOD TO THE PROBLEM OF HEAT TRANSFER IN A FREEZING SHAFT WALL(U) COLD REGIONS RESEARCH AND ENGINEERING LAB HANOVER NH F LIANDI AUG 86 CRREL-86-8 1/1

UNCLASSIFIED F/G 13/2 NL

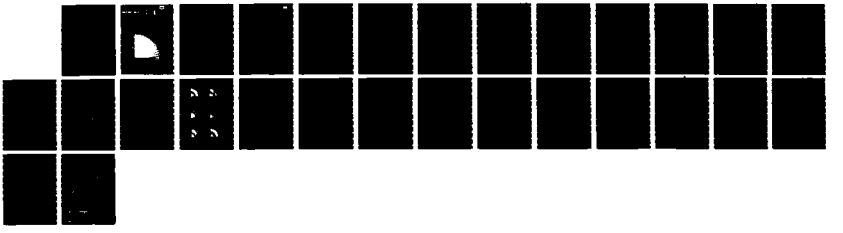

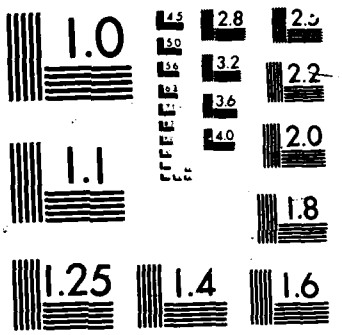
1.0
1.1
1.25
1.4
1.6
1.8
2.0
2.2
2.8
3.2
3.6
4.0

CRREL REPORT 86-8

US Army Corps of Engineers
Cold Regions Research & Engineering Laboratory

Applications of the finite-element method to the problem of heat transfer in a freezing shaft wall

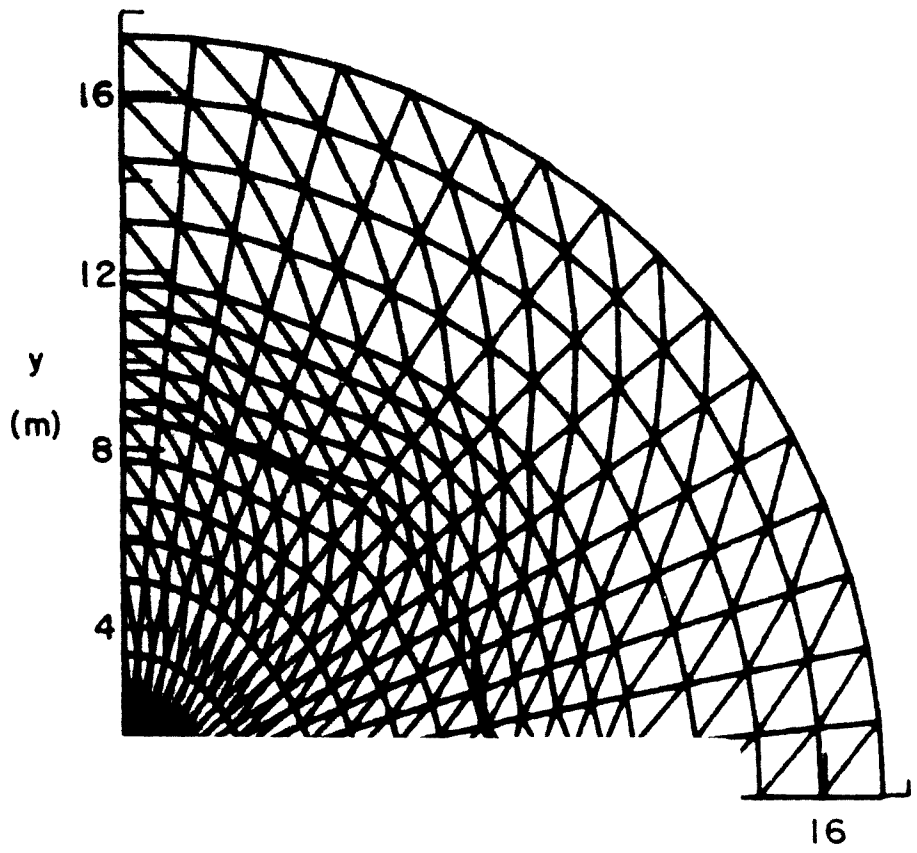

For conversion of SI metric units to U.S./British customary units of measurement consult ASTM Standard E380, Metric Practice Guide, *published by the American Society for Testing and Materials, 1916 Race St., Philadelphia, Pa. 19103.*

CRREL Report 86-8

August 1986

Applications of the finite-element method to the problem of heat transfer in a freezing shaft wall

Fu Liandi

Prepared for
OFFICE OF THE CHIEF OF ENGINEERS

Unclassified

SECURITY CLASSIFICATION OF THIS PAGE *(When Data Entered)*

REPORT DOCUMENTATION PAGE	READ INSTRUCTIONS BEFORE COMPLETING FORM
1. REPORT NUMBER CRREL Report 86-8	2. GOVT ACCESSION NO. AD-A172552
3. RECIPIENT'S CATALOG NUMBER	
4. TITLE *(and Subtitle)* APPLICATIONS OF THE FINITE-ELEMENT METHOD TO THE PROBLEM OF HEAT TRANSFER IN A FREEZING SHAFT WALL	5. TYPE OF REPORT & PERIOD COVERED
	6. PERFORMING ORG. REPORT NUMBER
7. AUTHOR(s) Fu Liandi	8. CONTRACT OR GRANT NUMBER(s)
9. PERFORMING ORGANIZATION NAME AND ADDRESS U.S. Army Cold Regions Research and Engineering Laboratory Hanover, New Hampshire 03755-1290	10. PROGRAM ELEMENT, PROJECT, TASK AREA & WORK UNIT NUMBERS Program Element 6.11.02A, DA Project 4A161102AT24, Task Area SS, Work Unit 009
11. CONTROLLING OFFICE NAME AND ADDRESS Office of the Chief of Engineers Washington, DC 20314	12. REPORT DATE August 1986
	13. NUMBER OF PAGES 31
14. MONITORING AGENCY NAME & ADDRESS *(If different from Controlling Office)*	15. SECURITY CLASS. *(of this report)* Unclassified
	15a. DECLASSIFICATION DOWNGRADING SCHEDULE

16. DISTRIBUTION STATEMENT *(of this Report)*

Approved for public release; distribution is unlimited.

17. DISTRIBUTION STATEMENT *(of the abstract entered in Block 20, if different from Report)*

18. SUPPLEMENTARY NOTES

19. KEY WORDS *(Continue on reverse side if necessary and identify by block number)*

Finite-element analysis
Freezing
Heat transfer
Soils
Tunnels

20. ABSTRACT *(Continue on reverse side if necessary and identify by block number)*

In this work, numerical computations of heat transfer for freezing a shaft wall have been conducted. Both fixed mesh and deforming mesh finite-element methods are used. In the fixed mesh method, latent heat effects are accounted for through a δ function in the apparent heat capacity. In the deforming mesh method, an automatic mesh-generation technique with transfinite mappings is used, and in this method two different approaches are taken to evaluate the movement of the interface. The freeze-pipes are considered as point sources with irregular distribution. The advancement of the inner and outer boundaries of the frozen wall is found to be in agreement with the previously computed results.

DD FORM 1 JAN 73 1473 EDITION OF 1 NOV 65 IS OBSOLETE

Unclassified

SECURITY CLASSIFICATION OF THIS PAGE *(When Data Entered)*

PREFACE

This report was prepared by Professor Fu Liandi of the Lanzhou Institute of Glaciology and Geocryology, Academia Sinica, during his one-year residence at CRREL at the expense of the Chinese government. Additional funding was provided by DA Project 4A161102AT24, *Research in Snow, Ice and Frozen Ground*, Task SS, *Combat Service Support*, Work Unit 009, *Phase Change Thermodynamics in Cold Regions Materials.*

This report was technically reviewed by Dr. Kevin O'Neill and Mary Albert of CRREL.

The author thanks William Quinn and Dr. Richard Berg for providing funding in connection with the numerical computation of this work. He expresses his sincere thanks to Dr. Kevin O'Neill for his kindness in providing pertinent literature and his technical discussions. He thanks Mary Albert for her helpful suggestions and extends his wholehearted thanks to Dr. Yin-Chao Yen for his invaluable help in this project and for his critical comments and suggestions in the preparation of this paper.

CONTENTS

ILLUSTRATIONS

Figure

TABLES

Table

Applications of the Finite-Element Method to the Problem of Heat Transfer in a Freezing Shaft Wall

FU LIANDI

INTRODUCTION

Artificial freezing has been widely used in the construction of trenches, tunnels, bridge openings and other underground structures. The essential problems with this technique are the determination of temperature change and the control of the freezing-thawing process in the developing frozen wall. The use of this technique is closely related to the engineering design, construction procedures, economic benefits and work safety.

In the area of Liang-Huai Coal Mine in China, the depth of the shaft is generally 300 to 700 m. For each shaft, about 40 freeze pipes are placed symmetrically along the circumference of radius R. The depth of the freeze pipe is usually identical to that of the shaft. The freeze pipes may also be staggered along two concentric circles, called freeze-pipe-circles, with radii R_1 and R_2. The coolant used for freezing is a brine solution with a temperature of approximately -30°C. By circulating the cold brine in pipes and the subsequent heat extraction between the pipe walls and soil, a frozen wall is thus formed. The process of frozen wall formation may be divided into four stages (Beijing Institute 1975).

In the first stage, which is called precircumscribed circling, freezing progresses radially at each freeze pipe, and a thin frozen wall will appear around each freeze pipe. After a certain duration that depends on the distance between every two adjacent freeze pipes and the specific flow condition of cold brine, all the small frozen walls will be connected to each other, and a global, nearly circular frozen wall will be formed.

After the formation of the global wall in the first stage, the frozen wall will concurrently grow inward and outward until its thickness and temperature reach desired values. This is called the active freezing stage.

During the third stage, continuous freezing is necessary to maintain an optimum thickness and temperature of the frozen wall while excavation and cement lining of the mine shaft are taking place. In the last stage, the circulation of cold brine is stopped as soon as the shaft work is completed. This is called the natural recovery period. Of the four stages, the active freezing stage is most important for predesigning. This paper will focus attention on this stage and try to calculate the change in the size of the frozen wall with the finite-element method.

A number of numerical methods have been used for solving heat transfer problems with phase change. The essential problem is to secure a solution for the moving boundary. The solution methods are usually divided into two basic types. The first type is represented by using traditional fixed mesh finite elements or finite differences where the phase front progresses through the stationary mesh and is interpolated with temperature distributions. Latent heat is handled with the methods of enthalpy or apparent heat capacity. In general, phase change occurs over a very narrow temperature range where enthalpy is represented by a steep line and apparent heat capacity has a peak value (Fig. 1; O'Neill 1983). An artificially extended temperature range ΔT is usually used to smooth the curves for both parameters. In practice, numerical results are sensitive to the selection of ΔT, and any unreasonable value of ΔT will introduce physical distortion.

O'Neill (1983) presented an approach for the case of two-dimensional problems; with the use of linear triangular elements, the effect of latent heat was included in apparent heat capacity, which is theoretically infinite at a discrete phase change temperature. Thus the artificially extended temperature range ΔT is not needed. This approach has the advantages of simplicity and efficiency.

The second type of solution method involves the use of a continuously deforming mesh, such that the phase boundary always lies on a particular numerical boundary. Because of the distinct boundary between the two phases, every element has its unique physical properties. Recently, Lynch and O'Neill (1981) and O'Neill and Lynch (1981) developed a method where finite differences in time are used and the mesh motion effects appear as a velocity term in the governing equation. This type of method is considered to be more flexible and accurate than the fixed mesh method and also capable of solving some special problems, e.g. the simulation of ice crystal growth and the process of icing of flowing water in a pipe (Sullivan et al. 1985, Albert 1984, Albert and O'Neill 1985). In this paper, both fixed and deforming mesh finite-element methods are used. In using the deforming mesh finite-element method, an automatic mesh-generation technique, transfinite mappings (Albert 1984) at each time step are adopted.

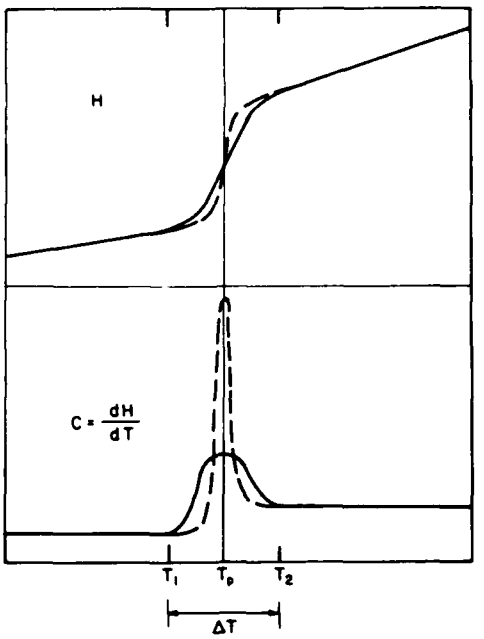

Figure 1. Enthalpy and apparent heat capacity curves over a temperature range.

BASIC FINITE-ELEMENT FORMULAS

Description of problem

Figure 2 shows a cross section of a cylindrical shaft, where r is the excavation radius and R the radius of freeze-pipe-circle. As is shown in the figure, neither the distance between adjacent pipes nor between the pipes and the center is equal. Consequently, the thickness of the global frozen wall is not uniform. During the active freezing stage, the global frozen wall will be advancing unevenly in both inward and outward directions.

The governing equation to be solved in each phase is the classical heat conduction equation:

$$C\frac{\partial T}{\partial t} = \nabla \cdot (K\nabla T) + Q \qquad (1)$$

with the interface boundary condition

$$L\frac{ds}{dt} = (K\nabla T)_f - (K\nabla T)_u \qquad (2)$$

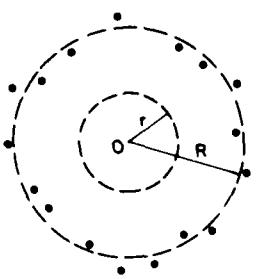

Figure 2. Distribution of freeze pipes.

where

T = temperature
t = time
C = volumetric heat capacity
K = heat conductivity
L = latent heat
s = position of phase boundary
Q = interior heat
f = frozen
u = unfrozen.

Finite-element equation–fixed mesh

Using the Galerkin finite-element method, we multiply eq 1 by a weighting function N_i and integrate over the whole domain A:

$$\int_A N_i \left[C \frac{\partial T}{\partial t} - \nabla \cdot (K \nabla T) - Q\right] dA = 0. \tag{3}$$

Integration of the second term by parts yields

$$\int_A [N_i C \frac{\partial T}{\partial t} + \nabla N_i \cdot K \nabla T] dA - \oint_{\Gamma_1} N_i K \frac{\partial T}{\partial n} d\gamma + \int_A Q N_i dA \tag{4}$$

where Γ_1 indicates the boundary with normal direction n. Now let the temperature be approximated as

$$T \approx \sum_{j=1}^{n} T_j(t) N_j(x, y). \tag{5}$$

Here N_j stands for the interpolating function, which is chosen to be the same as the weighting function N_i.

Substituting eq 5 in eq 4 gives

$$\frac{dT_j}{dt} \int_A C N_i N_j dA + T_j \int_A \nabla N_i \cdot K \nabla N_j dA - \oint_{\Gamma_1} N_i K \frac{\partial T}{\partial n} d\gamma + \int_A Q N_i dA = 0. \tag{6}$$

Discarding the term containing the integration of boundary heat flux and writing eq 6 in matrix notation, it becomes

$$[A] \left\{\dot{T}\right\} + [K] \left\{T\right\} + \left\{F\right\} = 0, \tag{7}$$

where

$$[A] = \int_A C N_i N_j dA$$

$$[K] = \int_A \nabla N_i \cdot K \nabla N_j dA$$

$$\left\{F\right\} = \int_A Q N_i dA.$$

The detailed derivation of $\left\{F\right\}$ is shown in Appendix A.

A key problem remaining to be solved is the integration of the integral that contains heat capacity C. To take into consideration the effect of latent heat L, O'Neill (1983) presented an application of a δ function by relating volumetric sensible heat c_s and latent heat L as

$$C = c_s + L\delta\,(T - T_p) \tag{8}$$

where C is the volumetric apparent heat capacity. It should be noted that with the use of a δ function, phase change will occur at a discrete temperature T_p.

Substituting eq 8 in eq 6, the first term gives

$$\int_A c_s N_i N_j dA + \int_A L N_i N_j \delta(T - T_p) dA. \tag{9}$$

The second term in eq 9 occurs only in the elements which contain the T_p isotherm, a detailed evaluation of which is shown in Appendix B. In the case of linear elements, K and c_s may be evaluated using the weighted area method.

Finite-element equation–deforming mesh

The Galerkin finite-element equation for deforming mesh takes the same form as eq 4:

$$\int_A \left[N_i\, C \frac{\partial T}{\partial t} + \nabla N_i \cdot K \nabla T\right] dA - \oint_{\Gamma_1} N_i K \frac{\partial T}{\partial n} d\gamma + \int_A Q N_i\, dA = 0. \tag{10}$$

But due to the deforming of the mesh with time, the interpolating function N_j is now a function of the mesh as well as time t. In a Cartesian system, let

$$T \approx \sum_{j=1}^{n} T_j(t)\, N_j(x, y, t). \tag{11}$$

Substituting eq 11 into eq 10, $\partial T/\partial t$ will yield two terms and eq 10 becomes

$$T_j \int_A K \nabla N_j \cdot \nabla N_i\, dA + T_j \int_A C N_i \frac{\partial N_j}{\partial t}\, dA + \frac{dT_j}{dt} \int_A C N_i N_j\, dA$$

$$- \oint_{\Gamma_1} N_i K \frac{\partial T}{\partial n} d\gamma + \int_A Q N_i\, dA = 0. \tag{12}$$

Lynch (1982) indicated that the value of $\partial N_j/\partial t$ is expressed in terms of V by

$$\frac{\partial N_j}{\partial t} = - V \cdot \nabla N_i \tag{13}$$

where $V = (d\mathbf{x}_i/dt)\psi_i$, $\mathbf{x}_i$ denotes the coordinates of nodes with respect to a fixed reference frame, ψ_i is the interpolating function and V is the mesh velocity. For the special case of linear triangular elements, $\psi_i = N_i$.

Substituting eq 13 in eq 12 gives

$$T_j \int_A K\nabla N_j \cdot \nabla N_i dA - T_j \int_A CN_i V \cdot \nabla N_j dA + \frac{dT_j}{dt} \int_A CN_i N_j dA$$

$$- \oint_{\Gamma_1} N_i K \frac{\partial T}{\partial n} d\gamma + \int_A QN_i dA = 0 . \tag{14}$$

$$[A]\left\{\dot{T}\right\} + [\kappa]\left\{T\right\} + \left\{F\right\} = 0 . \tag{15}$$

Equations 15 and 7 are in the same form, but the difference between them is in the representation of $[K]$. $[K]$, in this case, is

$$[K] = \int_A K\nabla N_j \cdot \nabla N_i dA - \int_A CN_i V \cdot \nabla N_j dA . \tag{16}$$

The solution of the second term in eq 16 is shown in Appendix C.

Equations 14 and 15 are the basic finite-element equations. To specify the motion of the phase front, two methods are used in this investigation.

Method 1

The following derivation appears as it was presented in Albert (1984). Equation 2 is the base for calculating the motion of phase boundary nodes. Since eq 2 cannot be exactly satisfied at a discretized boundary, Lynch (1982) proposed the use of a weaker integral form of eq 2:

$$\int_{\Gamma_2} L\left(\frac{ds}{dt}\right)_j N_j \cdot \mathbf{n} d\gamma = \int_{\Gamma_2} \left(K\nabla T\right)_f \cdot \mathbf{n} d\gamma - \int_{\Gamma_2} \left(K\nabla T\right)_u \cdot \mathbf{n} d\gamma$$

$$= \int_{\Gamma_2} \left(K\nabla T\right)_f \cdot \mathbf{n}\Sigma N_j d\gamma - \int_{\Gamma_2} \left(K\nabla T\right)_u \cdot \mathbf{n}\Sigma N_j d\gamma \tag{17}$$

where $\Sigma N_j = 1$, j refers to nodes on the phase boundary, $\mathbf{n}$ is the unit vector directed away from the frozen zone, and the integration is over the phase boundary Γ_2. If we now consider each boundary node j, eq 17 may be written

$$L\left(\frac{ds}{dt}\right)_j \cdot \int_{\Gamma_2} \mathbf{n} N_j d\gamma = \int_{\Gamma_2} \left[\left(K\frac{\partial T}{\partial n}\right)_f - \left(K\frac{\partial T}{\partial n}\right)_u\right] N_j d\gamma \tag{18}$$

where $\partial T/\partial n$ is the temperature gradient normal to the local boundary and $(ds/dt)_j$ is the velocity of node j with the unit vector $\mathbf{m}_j$. By using the characteristics of linear triangular elements and representing two adjacent sides of node j with length ℓ_1 and ℓ_2, we have

$$\int_{\Gamma_2} \mathbf{n} N_j d\gamma = \tfrac{1}{2}\,\ell_1\,\mathbf{n}_1 + \tfrac{1}{2}\,\ell_2\,\mathbf{n}_2 \tag{19}$$

and

$$V_j = \left(\frac{ds}{dt}\right)_j = \frac{1}{L} \frac{\ell_1\left[\left(K\frac{\partial T}{\partial n}\right)_{f_1} - \left(K\frac{\partial T}{\partial n}\right)_{u_1}\right] + \ell_2\left[\left(K\frac{\partial T}{\partial n}\right)_{f_2} - \left(K\frac{\partial T}{\partial n}\right)_{u_2}\right]}{\ell_1\,\mathbf{m}_j \cdot \mathbf{n}_1 + \ell_2\,\mathbf{m}_j \cdot \mathbf{n}_2} . \tag{20}$$

The magnitude of V_j may be evaluated from eq 20 if $\mathbf{m}_j$ is specified. To circumvent this difficulty, $\mathbf{m}_j$ is assumed to be a weighted average of $\mathbf{n}_1$ and $\mathbf{n}_2$:

$$\mathbf{m}_j = \frac{\mathbf{m}_j}{|\mathbf{m}_j|}, \text{ where } \mathbf{m}_j = \frac{\ell_1 \mathbf{n}_1 + \ell_2 \mathbf{n}_2}{\ell_1 + \ell_2}. \tag{21}$$

It should be noted that the direction of $\mathbf{m}_j$ can be chosen at one's convenience; consequently the magnitude of V_j will be in the chosen direction (App. D demonstrates this procedure).

Method 2

In a later paper, Lynch (1983) pointed out the deficiency of method 1 and reported a complete heat conservation method. The refined basic Galerkin equation is

$$\int_A C \frac{\partial T}{\partial t} N_i dA + \int_A K \nabla T \cdot \nabla N_i dA + \int_A Q N_i dA = F_i \tag{22}$$

where F_i includes two components, $F_i^{\Gamma_1}$ and $F_i^{\Gamma_2}$, which are the integrals of heat flux over the element and phase boundaries respectively, i.e.

$$F_i = F_i^{\Gamma_1} + F_i^{\Gamma_2} = \oint_{\Gamma_1} K \nabla T \cdot \mathbf{n} N_i d\gamma + \int_{\Gamma_2} \left[\left(K \nabla T \right)_f - \left(K \nabla T \right)_u \right] \cdot \mathbf{n} N_i d\gamma \tag{23}$$

The node motion on the phase boundary was evaluated through the combination of eq 18, 22, and 23 to form a complete heat conservation equation:

$$\int_A C \frac{\partial T}{\partial t} N_i dA + \int_A K \nabla T \cdot \nabla N_j dA + \int_A Q N_i dA$$

$$= \oint_{\Gamma_1} K \left(\frac{\partial T}{\partial n} \right) N_i d\gamma + L V_i \int_{\Gamma_2} n N_i d\gamma. \tag{24}$$

Lynch (1983) showed that the new phase boundary condition yields second-order accuracy and is easy to implement without extra computational difficulties (App. E shows the computational procedure).

TRANSFINITE MAPPING TECHNIQUE

In both of the deforming mesh methods used here, the interior mesh motion is governed by a mesh generation technique. Albert (1984) reviewed such techniques and demonstrated the usefulness of transfinite mappings (Haber et al. 1981) in conjunction with moving meshes. The interior mesh motion in this work is based on the method presented by Albert (1984).

In this method, we introduce a concept of a lofting projector P which maps a true surface to an approximate surface with a linear interpolatory constraint. In Figure 3, ψ_1, ψ_2 and ξ_1, ξ_2 are four curvilinear boundaries of a plane region, and we have a bilinear projector:

$$P(u,v) = (1-v)\psi_1(u) + v\psi_2(u) + (1-u)\xi_1(v) + u\xi_2(v)$$

$$- (1-u)(1-v)F(0,0) - (1-u)vF(0,1)$$

$$- uvF(1,1) - u(1-v)F(1,0)$$

$$0 \leq u \leq 1, \quad 0 \leq v \leq 1 \tag{25}$$

where u and v are normalized coordinates that change linearly along ψ_1, ψ_2 and ξ_1, ξ_2, respectively. For a three-sided region containing curvilinear boundaries ψ, ξ and η, the trilinear projector is

$$P(u,v,w) = \tfrac{1}{2}\left[\left(\frac{u}{1-v}\right)\psi(v) + \left(\frac{w}{1-v}\right)\eta(1-v) + \left(\frac{v}{1-w}\right)\eta(w)\right.$$

$$+ \left(\frac{u}{1-w}\right)\psi(1-w) + \left(\frac{w}{1-u}\right)\psi(u) + \left(\frac{v}{1-u}\right)\psi(1-u)$$

$$- w\psi(0) - u\xi(0) = v\eta(0)$$

$$0 \leq u \leq 1, 0 \leq v \leq 1, 0 \leq w \leq 1 \text{ and } u + v + w = 1 . \qquad (26)$$

As before, u, v and w are normalized coordinates that change linearly along ψ, ξ and η.

Applying eq 25 and 26, the boundaries of plane region may be divided into any number of discrete points as well as unevenly located. The trilinear projector results in triangular elements directly, while the bilinear projector forms unit squares that can be transformed to triangular elements with diagonals. In principle, eq 25 and 26 may be applied to any plane region of complex shape. This is done by dividing the whole region into a number of sub-regions. On occasion, it is more convenient to use bilinear and trilinear projectors to deal with three- and four-sided regions respectively. Albert (1984) discusses the use of these projectors and provides guidance on situations where they may fall.

At the end of each time step, a new mesh is generated with reference to the new phase front and other boundaries, and which forms the basis of the computation for the next time step.

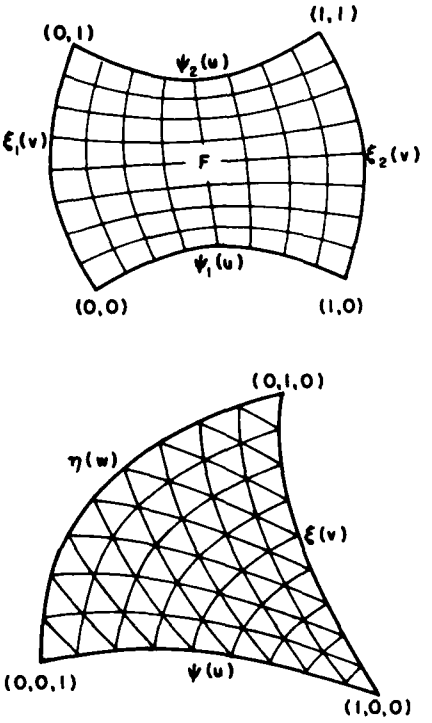

Figure 3. Mesh generation with transfinite mappings.

COMPUTATIONS AND CONCLUSIONS

In this investigation, only a quarter of a circular region with ten freeze-pipes is modeled. The physical parameters used here are obtained from the Panji-3 Dong Feng Shaft of the Liang-Huai Coal Mine in eastern China (Table 1).

The two straight boundaries of the computational region are specified to be zero-flux boundary conditions. In deforming mesh approach, the outer boundary nodes are kept at a constant temperature and moved outward at each time step. The extent of this movement is always twice that of the phase boundary.

Three programs were used: FEFIX performs the fixed mesh finite-element calculations as presented by O'Neill, MOVGR uses the moving mesh with transfinite mappings as presented by Albert (1984), and MOVHE incorporates the improvement over Albert's method suggested by Lynch. The flow charts of the programs are shown in Appendix F. For FEFIX, MOVHE and MOVGR, there are 42, 20 and 13 time steps adapted to simulate a period of 330 days. The program MOVGR iterates once on the location of phase front for each time step. In all the three programs, the parameter for implicitness in time θ is equal to 1.0; i.e. it is fully implicit.

Table 1. Parameters used in calculations.

Initial temperature,	T_o = 15°C
Boundary temperature,	T_b = 15°C
Phase change temperature,	T_p = 0°C
Heat conductivity,	K_u = 1.00 kcal/m · hr · °C
	K_f = 1.50 kcal/m · hr · °C
Heat capacity,	C_u = 710 kcal/m³ · °C
	C_f = 560 kcal/m³ · °C
Latent heat,	$L = 80 \cdot D(W-W_u)$
Dry density,	D = 1360 kg/m³
Relative water content,	W = 26.5%
Relative unfrozen water content,	W_u = 5%
Heat flux on pipe wall,	$Q = Q_T \cdot at^b$, $Q_T = 250\,\pi d$
Diameter of freeze-pipe,	d = 0.127 m
Statistical coefficients,	a = 4.08
	b = -0.28

Figure 4 shows the structure of fixed mesh and Figures 5, 6 and 7 illustrate the locations of phase fronts at 90, 210 and 330 days respectively. Similarly, for the deforming mesh used with method 1 and method 2, the phase boundaries for identical periods of 90, 210 and 330 days are shown in Figures 8, 9 and 10 and Figures 11, 12 and 13, respectively. Figure 14 shows the comparison of thickness of inner and outer frozen wall as a function of duration of operation among the computational methods. Figure 15 shows the growth of total frozen wall thicknesses as a function of time. The numerical results are also shown in Table 2. All the results in Figures 14 and 15 and in Table 2 are average values of frozen thickness at each time step.

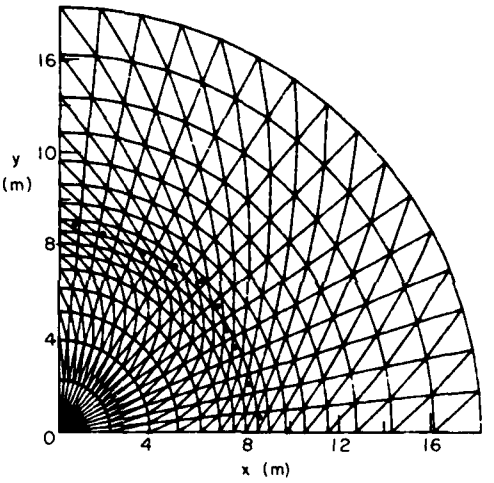

Figure 4. Fixed mesh and freeze-pipe distribution (FEFIX).

In practice, the fixed mesh method is found to be easier to program and takes much less CPU time than the deforming mesh method during the run. It is unfortunate that, because of the absence of experimental data and analytical solution, the computed results can only be compared with those reported by Ding et al. (1982) using the finite difference method and under the same physical conditions. The results of Ding have been compared with the field results and have been proved to be in good agreement.

Table 2. Computed thicknesses of frozen wall.

	Time (90 days)			*Time (150 days)*			*Time (210 days)*			*Time (270 days)*			*Time (300 days)*		
	Thickness (m)			*Thickness (m)*			*Thickness (m)*			*Thickness (m)*			*Thickness (m)*		
Program	*Inner*	*Outer*	*Total*	*Inner*	*Outer*	*Total*	*Inner*	*Outer*	*Total*	*Inner*	*Outer*	*Total*	*Inner*	*Outer*	*Total*
FEFIX	1.26	1.12	2.38	1.98	1.67	3.65	2.71	2.13	4.84	3.37	2.52	5.89	3.80	2.74	6.54
MOVGR	1.36	1.20	2.56	2.05	1.78	3.83	2.69	2.28	4.97	3.31	2.74	6.05	3.62	2.95	6.57
MOVHE	1.34	1.19	2.53	2.04	1.75	3.79	2.70	2.23	4.93	3.34	2.66	6.00	3.65	2.86	6.51
FINITE DIFFERENCE	1.50	1.36	2.86	2.10	1.83	3.93	2.70	2.28	4.98	3.30	2.65	5.95	3.60	2.82	6.42

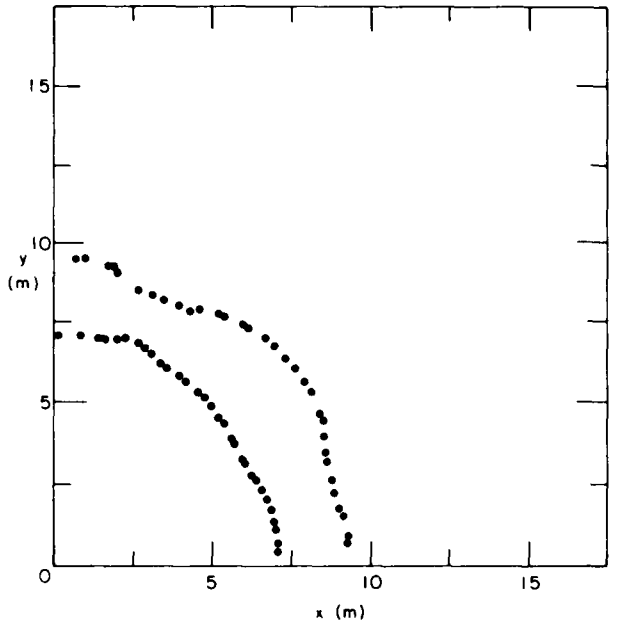

Figure 5. Locations of phase fronts at 90 days (FEFIX).

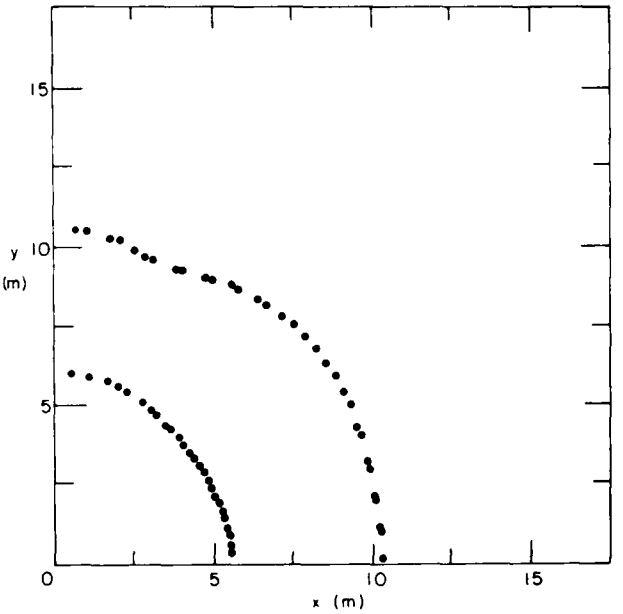

Figure 6. Locations of phase fronts at 210 days (FEFIX).

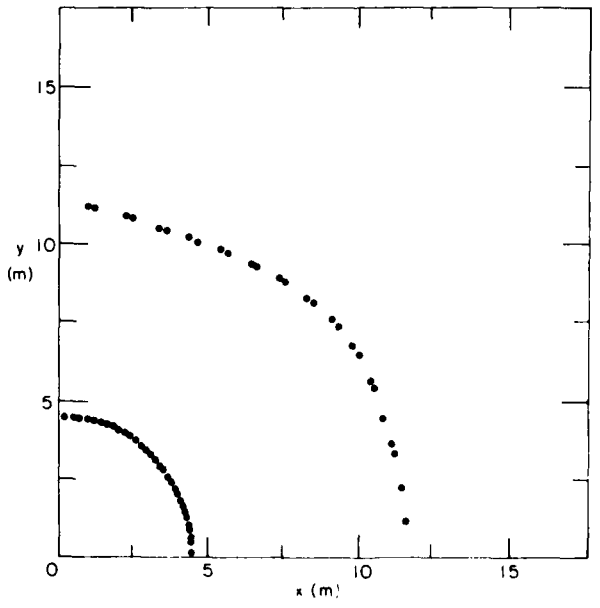

Figure 7. Locations of phase fronts at 330 days (FEFIX).

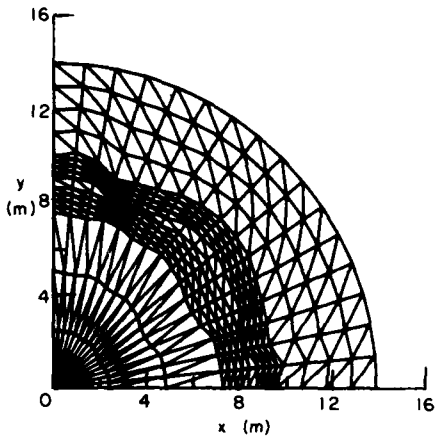

Figure 8. Deforming mesh at 90 days (MOVGR).

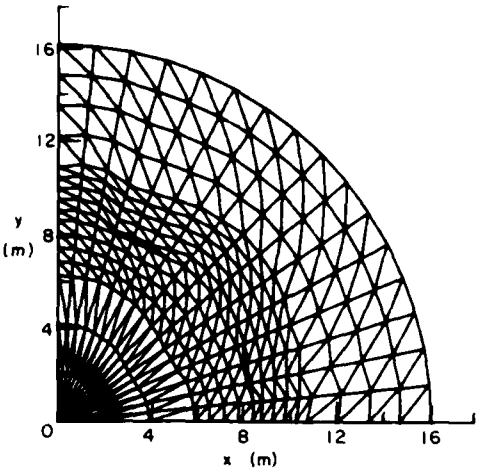

Figure 9. Deforming mesh at 210 days (MOVGR).

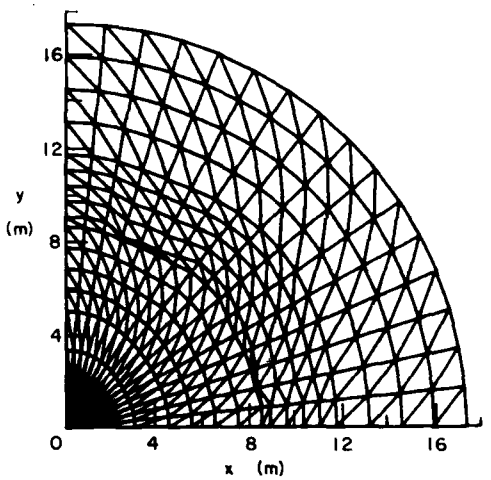

Figure 10. Deforming mesh at 330 days (MOVGR).

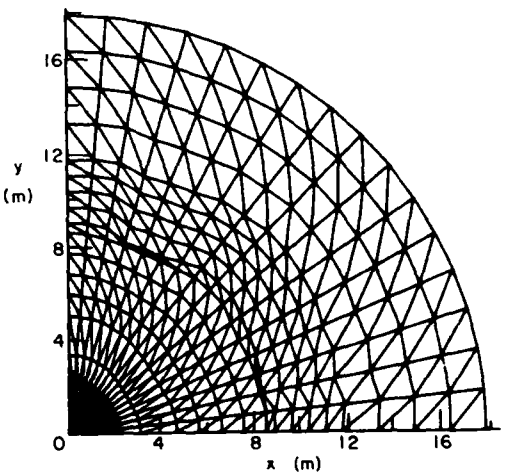

Figure 11. Deforming mesh at 90 days (MOVHE).

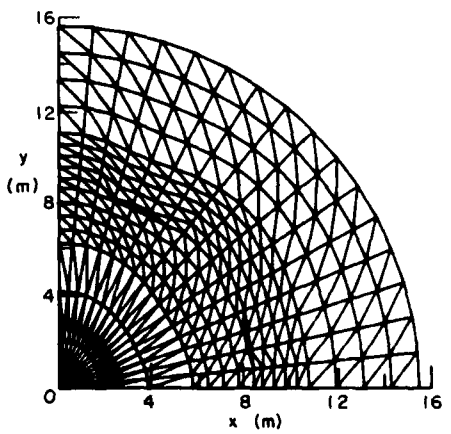

Figure 12. Deforming mesh at 210 days (MOVHE).

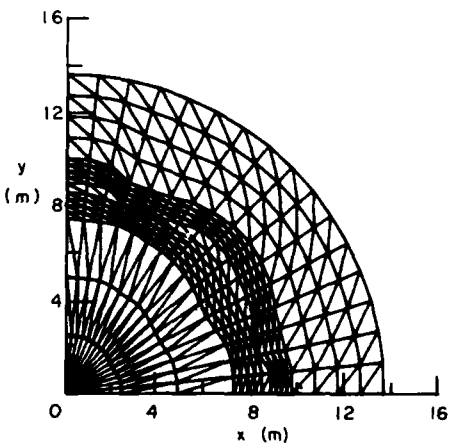

Figure 13. Deforming mesh at 330 days (MOVHE).

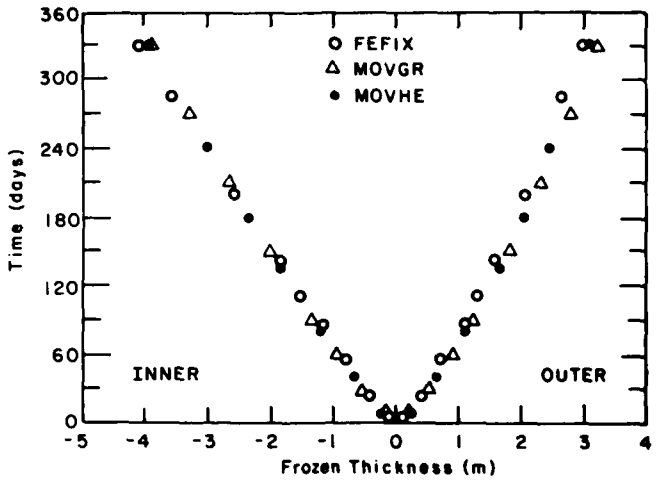

Figure 14. Changes in inner and outer thickness.

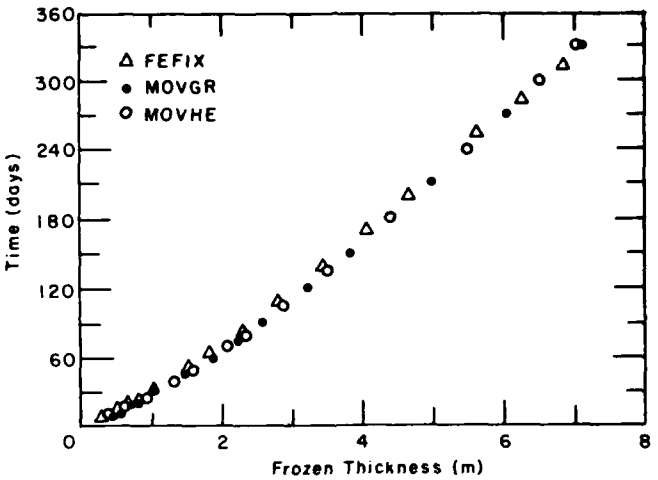

Figure 15. Changes in total frozen thickness.

LITERATURE CITED

Albert, M.R. (1984) Modeling two-dimensional freezing using transfinite mapping and a moving-mesh finite element technique. CRREL Report 84-10.

Albert, M.R. and K. O'Neill (1985) Transient two-dimensional phase change with convection, using deforming finite elements. *Recent Advances in Computational Heat Transfer*, New York: Wiley.

Beijing Institute, Shaft Construction Department, Coal Science Academy (1975) Shaft construction with artificial freezing method in coal mines. Coal Industry Publishing House.

Ding Dewen, Fu Liandi and Pang Rongqing (1982) The mathematical model of the change in artificially freezing wall and its calculation. *Science Bulletin*, China, **14**: 875-879.

Haber, R., M.S. Shepard, J.F. Abel, R.H. Galagher and D.P. Greenberg (1981) A general, two-dimensional, graphical finite element preprocessor utilizing discrete transfinite mappings. *International Journal for Numerical Methods in Engineering*, 17: 1015-1044.

Lynch, D.R. (1982) Unified approach to simulation on deforming elements with application to phase change problems. *Journal of Computational Physics*, 47: 387-411.

Lynch, D.R. and K. O'Neill (1981) Continuously deforming finite elements for the solution of parabolic problem, with and without phase change. *International Journal for Numerical Methods in Engineering*, 17: 81-96.

Lynch, D.R. (1983) Heat conservation in deforming element phase change simulation. *Journal of Computational Physics.*

O'Neill, K. and D.R. Lynch (1981) A finite element solution for freezing problems, using a continuously deforming coordinate system. *Numerical Methods in Heat Transfer* (R. Lewis, K. Morgan, O.C, Zienkiewicz, Eds.), New York: John Wiley and Sons.

O'Neill, K. (1983) Solution of two-dimensional axisymmetric phase change problems on a fixed mesh, with zero width phase change zone. *Proceedings, 3rd International Conference on Numerical Methods in Thermal Problems*, Seattle.

Segerlind, L.J. (1984) Applied finite element analysis. Second Edition, New York.

Sullivan, J.M., D.R. Lynch and K. O'Neill (1985) Finite element simulation of ice crystal growth in subcooled sodium-chloride solutions. *Proceedings, International Conference on Advanced Numerical Methods in Engineering*, Swansea, U.K.

APPENDIX A: POINT HEAT SOURCES.

In eq 7 and 15,

$$\{F\} = \int_A QN_i dA \tag{A1}$$

For elements containing freeze-pipe, the heat source Q is treated as a point source and by introducing δ functions (Segerlind 1984), eq 1 becomes

$$\int_A QN_i \delta (x - x_o) \delta (y - y_o) dxdy \tag{A2}$$

where (x_o, y_o) is the coordinate of freeze-pipe. Thus we have

$$\{F\} = Q \begin{Bmatrix} N_i(x_o, y_o) \\ N_j(x_o, y_o) \\ N_k(x_o, y_o) \end{Bmatrix} \tag{A3}$$

where i, j, k denote the three nodes of the element. By using eq A3, the effect of Q may be automatically distributed to neighboring nodes, depending on the relative location from the point (x_o, y_o).

APPENDIX B: EVALUATION OF THE INTEGRAL INCLUDING LATENT HEAT (FIXED MESH).

The integral including latent heat is

$$\int_A L\, N_i N_j \delta (T - T_p)\, dxdy. \tag{B1}$$

To integrate this, one of the spatial variables must be expressed in terms of T. In Figure B1, the isotherm crosses the element and intersects with two of the sides at points 1 and 2. Let the new coordinate system be (x', y'), where y' extends along the isotherm, and x' is perpendicular to the isotherm. Equation 1 becomes

$$\int_A L\, N_i N_j \delta\, (T - T_p)\, dx'dy'\,. \tag{B2}$$

where N_i and N_j are the functions of x' and y'. Thus all isotherms in the element are parallel to y', T is only a function of x' and dx' is $(dx'/dT) \cdot dT$. Therefore eq B2 can be written as

$$\int_{y'} \int_T L\, N_i N_j \delta\, (T - T_p) \frac{dx'}{dT}\, dTdy' \tag{B3}$$

where dx'/dT, the reciprocal of temperature gradient along x', is a constant. Applying the character of δ function, eq B3 becomes

$$L \frac{dx'}{dT} \int_{y'_1}^{y'_2} N_i N_j \Big|_{T = T_p} dy'\,. \tag{B4}$$

Equation B4 is a line integral along the isotherm. Using Simpson's rule, eq B4 becomes

$$L \frac{dx'}{dT} \cdot \frac{\ell}{6} (2N_{i1} N_{j1} + 2N_{i2} N_{j2} + N_{i1} N_{j2} + N_{i2} N_{j1}) \tag{B5}$$

where

$$\frac{dx'}{dT} = 1/\frac{dT}{dx'} = 1/\sqrt{\left(\frac{\partial T}{\partial x}\right)^2 + \left(\frac{\partial T}{\partial y}\right)^2}$$

and

$$\frac{\partial T}{\partial x} = (b_i T_i + b_j T_j + b_k T_k)/2A$$

$$\frac{\partial T}{\partial y} = (c_i T_i + c_j T_j + c_k T_k)/2A\,. \tag{B6}$$

ℓ represents the length of isotherm, which can be evaluated geometrically. The values of N_{i1}, N_{i2}, N_{j1} and N_{j2} can easily be specified because of the properties of interpolation functions, and in eq B6, i, j and k denote element nodes.

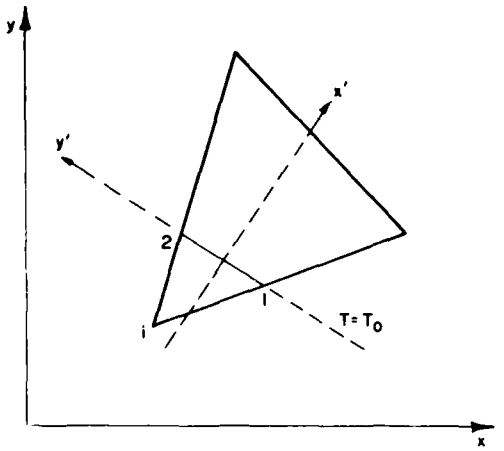

Figure B1. Evaluation of the integral including latent heat.

APPENDIX C: SPECIFICATION OF $[K]$ –DEFORMING MESH.

There are two terms in $[K]$. One of the terms is

$$\int_A CN_i V\cdot\nabla N_j dA \tag{C1}$$

where C is constant for any element at each time step, and $V\cdot\nabla N_j$ may be written as $V_\ell\, \partial N_j/\partial x_\ell$

$$\frac{\partial N_j}{\partial x_\ell} = \frac{1}{2A}\begin{bmatrix} b_i & b_j & b_k \\ c_i & c_j & c_k \end{bmatrix} \tag{C2}$$

where ℓ denotes x and y, and i, j and k denote three nodes. V_ℓ can be written as

$$V_\ell = \begin{bmatrix} V_{xi} & V_{yi} \\ V_{xj} & V_{yj} \\ V_{xk} & V_{yk} \end{bmatrix} \tag{C3}$$

where V_{xi}, V_{yi} and so on can be calculated from node locations for the two meshes representing the region at the beginning and end of the time step. Using eq C2 and C3 in eq C1, we have

$$CV_\ell \nabla N_j \int_A N_i N_j dA\,. \tag{C4}$$

APPENDIX D: SPECIFYING $\partial T/\partial n$ AND THE DIRECTION OF m_j FOR METHOD 1.

When the radial direction of m_j is specified, the solution of $\ell_1 m_j \cdot n_1$ and $\ell_2 m_j \cdot n_2$ may be implemented geometrically. In Figure D1,

$$m_j \cdot n_1 = |m_j| \cdot |n_1| \cdot \cos\beta = d_1/d_2$$

$$\ell_1 m_j \cdot n_1 = |(x_{j-1}-x_j)y_i - (y_{j-1}-y_j)x_i + (x_j y_{j-1} - x_{j-1} y_j)| / \sqrt{(x_j-x_i)^2 + (y_j-y_i)^2} \quad . \qquad \text{(D1)}$$

$\ell_2 m_j \cdot n_2$ can be evaluated in the same manner.

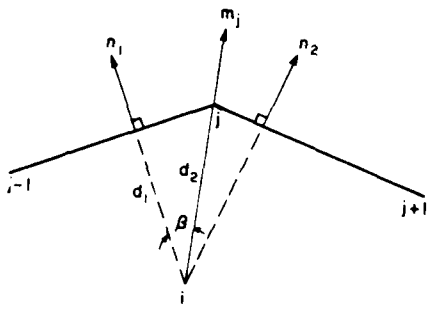

Figure D1. Specification of the motion of node j *on phase boundary.*

$\partial T/\partial n$ is the temperature gradient normal to phase boundary. In eq 2 (in text), $\partial T/\partial n$ contains four terms referring to the adjacent two sides and to the frozen and unfrozen zones respectively. Each may be specified with the following equation:

$$\frac{\partial T}{\partial n} = \sqrt{\left(\frac{\partial T}{\partial x}\right)^2 + \left(\frac{\partial T}{\partial y}\right)^2} \quad . \qquad \text{(D2)}$$

APPENDIX E: PROCEDURES OF METHOD 2.

The complete heat conservation equation (eq 24) (in text) may be written in matrix notation:

$$\left\{S_i\right\} = \frac{2}{L} \frac{[M]\left\{T\right\}^{n+1} - \{N\}}{\ell_1 n_1 + \ell_2 n_2} \tag{E1}$$

where

$$[M] = [A] + \theta \Delta t [k]$$

$$\left\{N\right\} = ([A] - (1-\theta)\Delta t[k])\left\{T\right\}^n + \Delta t[(1-\theta)\left\{F\right\}^n + \theta\left\{F\right\}^{n+1}] .$$

The procedure for computing $\left\{S_i\right\}$ is as follows:

1, Form global equations as usual.
2, Save the equations of phase boundary nodes, i.e. $[M]$ and $\left\{N\right\}$.
3, Solve the nodal temperature.
4, Compute the latent heat balance with the saved equations in step 2 and the new temperature found in step 3.

APPENDIX F: EXPLANATION OF PROGRAMS.

(A) Name

FEFIX – Fixed mesh finite element method (flow chart in Figure F1).

MOVGR – Deforming mesh with method 1 (flow chart in Figure F2).

MOVHE – Deforming mesh with method 2 (flow chart in Figure F3).

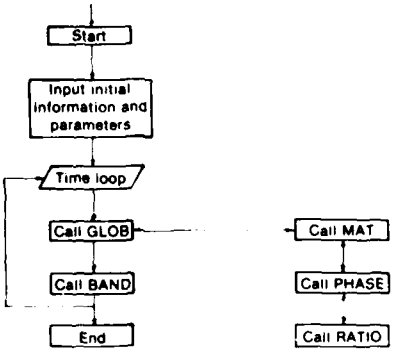

Figure F1. Flow chart for FEFIX.

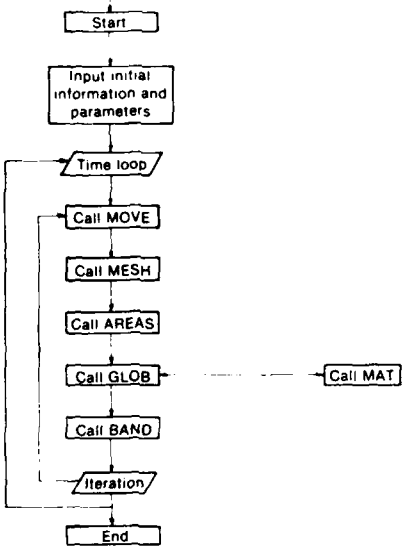

Figure F2. Flow chart for MOVGR.

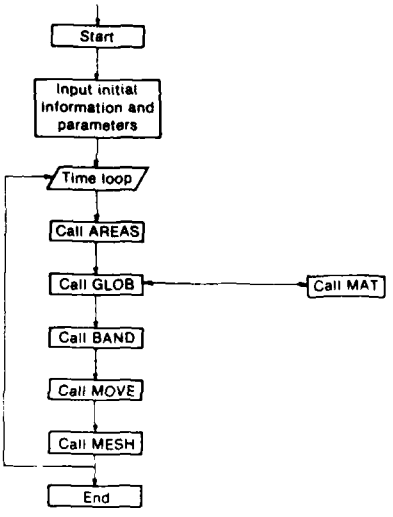

Figure F3. Flow chart for MOVHE.

(B) FEFIX

FEFIX contains the main program and subroutines GLOB, MAT, PHASE, RATIO and BAND.

GLOB – Forms global matrices and inserts boundary conditions.

MAT – Specifies the element matrices.

PHASE – Specifies the location of the T_p isotherm.

RATIO – Specifies parameters K and C in the elements containing phase change.

BAND – Solves symmetric, banded and positive definite matrix equations and obtains nodal temperatures.

(C) MOVGR

MOVGR contains main program and subroutines MOVE, MESH, AREAS, GLOB, MAT and BAND.

MOVE -- Specifies the motions of phase boundary nodes with method 1.

MESH – Generates a new mesh using the new locations of phase boundaries and transfinite mappings. The velocities of nodal motion are calculated from the locations of new and old meshes.

AREAS – Specifies new element areas at each time step.

GLOB – Forms global matrices and inserts boundary conditions.

MAT – Specifies the element matrices.

BAND – Solves banded and positive definite matrix equations and obtains nodal temperatures.

(D) MOVHE

MOVHE contains main program and subroutines MOVE, MESH, AREAS, GLOB, MAT and BAND. In the subroutines, only MOVE and GLOB are different from those in MOVGR.

MOVE – Specifies the motions of phase boundary nodes with method 2, in which the saved nodal equations are used.

GLOB -- Forms global matrices, inserts boundary conditions and saves the nodal equations on phase boundary.

A facsimile catalog card in Library of Congress MARC format is reproduced below.

Fu Liandi

Applications of the finite-element method to the problem of heat transfer in a freezing shaft wall / by Fu Liandi. Hanover, N.H.: Cold Regions Research and Engineering Laboratory; Springfield, Va.: available from National Technical Information Service, 1986.

iii, 31 p., illus.; 28 cm. (CRREL Report 86-8.)

Prepared for Office of the Chief of Engineers by Corps of Engineers, U.S. Army Cold Regions Research and Engineering Laboratory .

Bibliography: p. 11.

1. Finite-element analysis. 2. Freezing. 3. Heat transfer. 4. Soils. 5. Tunnels. I. United States. Army. Corps of Engineers. II. Cold Regions Research and Engineering Laboratory, Hanover, N.H. III. Series: CRREL Report 86-8.

END

11-86

DTIC